Check for updates

Received: 8 May 2023 | Accepted: 10 September 2023

DOI: 10.1111/1365-2656.14008

Journal of Animal Ecology | BRITISH ECOLOGICAL SOCIETY

RESEARCH ARTICLE

Effects of local density dependence and temperature on the spatial synchrony of marine fish populations

Jonatan F. Marquez[1,2] | Ivar Herfindal[1,3] | Bernt-Erik Sæther[1,3] | Sondre Aanes[4] | Are Salthaug[2] | Aline Magdalena Lee[1,3]

[1]Department of Biology, Centre for Biodiversity Dynamics, Norwegian University of Science and Technology, Trondheim, Norway

[2]Institute of Marine Research, Bergen, Norway

[3]Gjærevoll Centre for Biodiversity Foresight Analyses, Norwegian University of Science and Technology, Trondheim, Norway

[4]Norwegian Computing Center, Oslo, Norway

Correspondence
Jonatan F. Marquez
Email: jonatan.fredricson@gmail.com

Funding information
Norges Forskningsråd, Grant/Award Number: 223257 and 244647

Handling Editor: Thierry Boulinier

Abstract

1. Disentangling empirically the many processes affecting spatial population synchrony is a challenge in population ecology. Two processes that could have major effects on the spatial synchrony of wild population dynamics are density dependence and variation in environmental conditions like temperature. Understanding these effects is crucial for predicting the effects of climate change on local and regional population dynamics.
2. We quantified the direct contribution of local temperature and density dependence to spatial synchrony in the population dynamics of nine fish species inhabiting the Barents Sea. First, we estimated the degree to which the annual spatial autocorrelations in density are influenced by temperature. Second, we estimated and mapped the local effects of temperature and strength of density dependence on annual changes in density. Finally, we measured the relative effects of temperature and density dependence on the spatial synchrony in changes in density.
3. Temperature influenced the annual spatial autocorrelation in density more in species with greater affinities to the benthos and to warmer waters. Temperature correlated positively with changes in density in the eastern Barents Sea for most species. Temperature had a weak synchronizing effect on density dynamics, while increasing strength of density dependence consistently desynchronised the dynamics.
4. Quantifying the relative effects of different processes affecting population synchrony is important to better predict how population dynamics might change when environmental conditions change. Here, high degrees of spatial synchrony in the population dynamics remained unexplained by local temperature and density dependence, confirming the presence of additional synchronizing drivers, such as trophic interactions or harvesting.

KEYWORDS
Barents Sea, density dependence, distribution, environmental sensitivity, local dynamics, spatial autocorrelation, spatial distribution, synchrony

This is an open access article under the terms of the Creative Commons Attribution-NonCommercial-NoDerivs License, which permits use and distribution in any medium, provided the original work is properly cited, the use is non-commercial and no modifications or adaptations are made.
© 2023 The Authors. *Journal of Animal Ecology* published by John Wiley & Sons Ltd on behalf of British Ecological Society.

1 | INTRODUCTION

The spatial dynamics of populations are influenced by a myriad of processes that need to be understood to allow predictions about how populations will respond to changes in environmental conditions, community composition, species interactions or population demographic structure (Planque et al., 2011). This can have important implications for conservation planning and harvesting strategies (Fogarty & Botsford, 2007). An important part of understanding spatial population dynamics is understanding spatial population synchrony, which refers to how population dynamics are correlated across space (Liebhold et al., 2004). Spatial synchrony in population dynamics plays a crucial role in ecology because high degrees of synchrony can be associated with greater rates in the spread of disease (Bjørnstad, 2000; Viboud et al., 2006), lower maximum sustainable yields (Engen, 2017) and higher probability that a species will be at low abundance across much of its range simultaneously, increasing its risk of extinction (Engen et al., 2002; Lande et al., 1999).

Three main non-mutually exclusive processes are known to cause spatial synchrony in population dynamics. First, spatially synchronous environmental variables, such as temperature or precipitation, can synchronise local dynamics across distant locations through what is known as the Moran effect (Cheal et al., 2007; Fay et al., 2020). Second, dispersal can connect local dynamics across space, homogenizing density within certain distances (Cheal et al., 2007; Vindstad et al., 2019). Third, population dynamics can be synchronised by density-dependent effects of trophic interactions when the interacting species is spatially synchronised itself (Turkia et al., 2020) or by a wide-ranging nomadic predator (Ims & Andreassen, 2000). Harvesting can have similar synchronizing effects on a population (Jarillo et al., 2020). These processes can be further influenced by, for instance, the strength of density dependence of a population (Lande et al., 1999), community complexity (Liu et al., 2016), spatial environmental heterogeneity (Engen & Sæther, 2005; Walter et al., 2017) and cyclicity in population dynamics (Bjørnstad, 2000), making the task of disentangling the effects of individual processes challenging.

Environmental variables can act as strong synchronizing agents (Hansen et al., 2020). The synchronizing effect of an environmental variable is limited to the range of the population that responds similarly to changes in that environmental variable (Lande et al., 1999; Moran, 1953). However, environmental effects on local dynamics often vary across the distribution ranges of populations (Walter et al., 2017). For example, high temperatures might have positive effects on population dynamics at the high latitudinal or altitudinal boundaries of a species' range, but negative effects around the lower latitudinal or altitudinal boundaries, where the individuals were already close to their thermal tolerance maxima (Poloczanska et al., 2013). Similarly, individuals at the latitudinal or altitudinal distributional margins are expected to be more influenced by key local environmental factors than individuals at the centre of the species distribution (Muffler et al., 2020; Myers, 1998; Walter et al., 2017). Thus, a synchronizing environmental condition might significantly synchronise only a portion of a population's distribution (Östman et al., 2017). In addition, environmental conditions can synchronise populations indirectly through their effects on quality and quantity of food resources (Grøtan et al., 2005), species assemblage (Liu et al., 2016) or dispersal (Vindstad et al., 2019). Such indirect effects are likely to also follow some spatial structures that are important to understand (Vindstad et al., 2019). As populations shift geographically due to globally changing climates (Sunday et al., 2012), the proportions of the populations exposed to key synchronizing environmental variables are likely to change too and thus their spatial population synchrony. It is therefore important to identify and quantify the effects of individual environmental variables on the synchrony of different populations in order to improve our understanding of how changes in environmental conditions might alter population dynamics.

Variation in the strength of density dependence, that is the inverse of the return time to the carrying capacity (May, 1974), can influence the level of synchrony among populations (Lande et al., 1999). High population densities increase intraspecific competition for limiting resources, decreases access to suitable living areas, attract more predators, and reduce habitat suitability, which in turn affects population dynamics by locally reducing reproductive rates and increasing mortality and emigration rates (Myers & Cadigan, 1993; Shepherd & Litvak, 2004). Species with strong density dependence respond to departures from population carrying capacity faster, while species with weaker density dependence respond more slowly (May, 1987). This allows an increase in density of a species with weaker density dependence to spread more and farther, less affected by local densities, thereby synchronizing dynamics across larger areas (Bjørnstad et al., 1999; Liebhold et al., 2004). In comparison, changes in local density in strong density-dependent species will be more rapidly regulated locally, limiting the chance of rippling effects across space, thus resulting in more asynchronous dynamics in space. The expected effects of density dependence on spatial synchrony have mostly been studied in metapopulations (e.g. Fay et al., 2020; Turkia et al., 2020; Vindstad et al., 2019), where each subpopulation represents a spatial unit, however, similar processes could take place within a continuously distributed population. Density regulating processes and the strength of density dependence can also vary spatially (Fromentin et al., 2001; Hugueny, 2006), for example, depending on local spatial predator–prey dynamics (Liu et al., 2016), habitat types or harvest pressure (Johnson, 2006; Thorson et al., 2015). Consequently, one might find areas within a species' distribution where individuals are subject to strong density dependence, generating asynchrony, and areas with weak density dependence which could promote synchrony.

Population dynamics and vital rates in marine fish are often spatially synchronised over great distances, with variation in the degree and spatial scale of synchrony depending on the habitat types, species and population age-structures (Cheal et al., 2007; Marquez et al., 2019; Morrongiello et al., 2021; Myers et al., 1997). Because of the large scales over which marine fish tend to be synchronised, highly synchronised environmental variables, like temperature, are

13652656, 2023, 11, Downloaded from https://besjournals.onlinelibrary.wiley.com/doi/10.1111/1365-2656.14008 by Institute Of Marine Research, Wiley Online Library on [21/11/2023]. See the Terms and Conditions (https://onlinelibrary.wiley.com/terms-and-conditions) on Wiley Online Library for rules of use; OA articles are governed by the applicable Creative Commons License

often argued to be the main spatially synchronizing drivers (Kleisner et al., 2010; Myers et al., 2015). Indeed, temperature influences fish body temperature and thereby metabolic-, digestive-, reproductive- and muscle movement rates, ultimately affecting natural mortality rates (Pauly, 1980), as well as other vital rates (Husson et al., 2020; Laurel et al., 2007; Morrongiello et al., 2021). However, while some studies have compared patterns of synchrony in temperature to synchrony in marine fish population dynamics (Cheal et al., 2007; Kleisner et al., 2010), to the best of our knowledge, none have quantified the direct effect of temperature on local dynamics to quantify actual impact.

Here, we study patterns of spatial autocorrelation in density and spatial synchrony in annual changes in density of nine marine fish species in the Barents Sea, and how these patterns are influenced by local temperature and geographical variation in the strength of density dependence. First, we quantify the effect of temperature on the spatial autocorrelation in density each year. Second, we examine how annual changes in population density are affected by local density dependence and temperature, and how these effects vary across the Barents Sea for each species. Third, we estimate the spatial synchrony in the annual changes in population density, and in the residual annual changes in density after accounting for the effects of (1) local temperature, (2) density dependence and (3) the combination of the two. We explore commonalities and differences between the patterns of spatial autocorrelation and synchrony, and among the nine study species.

2 | MATERIALS AND METHODS

2.1 | Study region and species

We examined the spatial density dynamics of nine species found within the Barents Sea: Beaked redfish (*Sebastes mentella*), blue whiting (*Micromesistius poutassou*), capelin (*Mallotus villosus*), cod (*Gadus morhua*), haddock (*Melanogrammus aeglefinus*), Norwegian spring-spawning herring (*Clupea harengus*), long rough dab (*Hippoglossoides platessoides*), lumpfish (*Cyclopterus lumpus*) and Norway pout (*Trisopterus esmarkii*). We focused on these species because, among the species collected by the Barents Sea annual bottom trawl survey (described in the following section), they were the only ones with sufficient continuous data across space and time to produce reliable estimates of population dynamics and density dependence. These species differ in key biological characteristics, such as foraging behaviour, reproductive tactics, diet, trophic level, and thermal and habitat preference (Aune et al., 2018; Eriksen et al., 2020; Husson et al., 2020). All species carry out annual spawning migrations to their respective spawning areas, mostly along the Norwegian coast, during the spring months (Olsen et al., 2010). Eggs and larvae are then transported by currents back into the Barents Sea. Variation in factors such as prevailing currents, sea temperature and vertical distribution of the larvae in the water column can have strong impacts on the cohort size at the end of the larvae stage, that is the year-class strength (Dingsør et al., 2007), which could have a synchronizing effect on density variation across the population in the following years. Cod, herring and beaked redfish exhibit strong spatial segregation between age classes, with adult herring and beaked redfish becoming mostly absent in the Barents Sea as they shift their distribution toward the North Atlantic upon reaching maturity (Huse et al., 2002; Planque et al., 2013). Since there is no direct local recruitment, the local variation in density studied here is assumed to be influenced by local mortality and migration rates, not local reproduction potential. For instance, areas with below average densities might successfully receive more recruits and immigrants. All studied species are subject to different degrees of harvesting pressure (Stiansen & Filin, 2008).

The Barents Sea is an Arcto-boreal continental shelf sea characterised by strong spatial and temporal environmental variability (Herfindal et al., 2022). Warm Atlantic waters enter the Barents Sea from the southwest and meet cold Arctic waters flowing in from the northeast, resulting in a strong thermal gradient. During the winter months, the Barents Sea is also largely covered by sea ice that melts gradually in a north-eastward direction during the spring. In turn, the melting of the sea ice has important effects on the ecological processes of the region, directly affecting primary productivity, fish recruitment and dispersal patterns (Olsen et al., 2010). The Barents Sea has been warming in recent decades, which has affected current strengths and the timing and rate of sea ice melting (Dalpadado et al., 2012). In turn, this is affecting the spatial distribution of many fish populations (Fossheim et al., 2015). While the Barents Sea hosts hundreds of fish species, the regional food web is relatively simple as it is dominated by interactions between a few highly abundant species (Eriksen et al., 2020).

2.2 | Data collection

We used fish data from annual scientific bottom trawl surveys conducted from 1985 to 2016, between January and March, by the Norwegian Institute for Marine Research and the Polar Research Institute of Marine Fisheries and Oceanography (Fall et al., 2020). The exact sampling locations vary between years, but the survey follows a spatially stratified sampling design with fairly consistent spatial coverage of the Barents Sea, with some exceptions caused by years of bad weather, extensive sea ice or limited access to Russian waters. Each sampling station was sampled with a Campelen 1800 demersal trawl with a mesh size of 22 mm on the cod-end, which was towed for 30 min, or 15 min after 2010, at a speed of 3 knots. The area covered by the trawls and the geometry of the trawl's mouth were monitored during towing with doppler logs or GPS and SCANMAR systems. The abundance of each species within the catch was sampled onboard following the protocols outlined in Mjanger et al., 2020. When the catch was excessively large a representative subsample of the catch was sampled, and the counts then scaled up to become representative of the entire catch. More details on the survey sampling design can be found in Fall et al., 2020 and Jakobsen et al., 1997. Finally, the density of

13652656, 2023, 11, Downloaded from https://besjournals.onlinelibrary.wiley.com/doi/10.1111/1365-2656.14008 by Institute Of Marine Research, Wiley Online Library on [21/11/2023]. See the Terms and Conditions (https://onlinelibrary.wiley.com/terms-and-conditions) on Wiley Online Library for rules of use; OA articles are governed by the applicable Creative Commons License

each species was estimated by dividing their overall catch within the trawl by the area trawled and standardizing to individuals per nautical mile. Sea temperature measurements were collected at each fish sampling site using a CTD-probe (Figure S1). Since the fish data were collected through bottom trawl surveys, we here used the average SBT (averaging the records within the 30 deepest meters). The data used for the study had been collected by a governmental institution for monitoring and research purpose, thus we did not need special ethical approvals nor fieldwork permissions.

2.3 | Data analyses

To analyse spatial patterns across the Barents Sea, the study region was overlaid with a hexagonal grid that subdivided it into similar sized cells (i.e. sites) with equidistant centroids to their neighbouring cells. Since the exact sampling locations were not consistent across or within years, the density of each species and temperature measurements obtained from each sampling station were averaged within its corresponding cell. Choice of grid resolution could be important in this type of study because fine resolutions result in more sites with incomplete time series and coarse resolutions increase the chance of missing a spatial signal within the data (Liebhold et al., 2012). Therefore, we assessed the influence of the grid resolution and placement by repeating the analyses at resolutions of 4900, 6400, 8100, 10,000 and 12,100 km^2, and by shifting the position of the grid latitudinally and longitudinal 25 times. We present the results from the analyses at 8100 km^2 resolution, corresponding to a separation between neighbouring centroids of ~95 km, because it presented a good balance between reducing the number of sites lost due to incomplete time series at finer resolutions and reducing the degree of uncertainty which increased at coarser resolutions, and previous studies in the region support this resolution (Marquez et al., 2019). The general results were consistent across resolutions (see Figure S5).

2.4 | Spatial autocorrelation

We used spatial variogram analyses to estimate the spatial autocorrelation in the annual density distribution of each species, before and after accounting for the estimated effects of temperature on density (Pebesma, 2004). First, annual local densities (N_t) of each species were log transformed to normalise their distribution, removing sites-years with zero density, thus making all results conditional on the presence of the species. We justify this decision by the fact that the presence of the species tended to occur mostly within continuous regions, causing most zeros to also occur in continuous regions outside the species core range, which might have erroneously inflated autocorrelation estimates. The transformed densities were modelled as a function of temperature, allowing the models' intercept to vary between years to account for changes in the overall population size. Temperature was allowed to have a quadratic effect, where density was expected to be highest at the species' thermal optimum and decline as temperature decreased or increased from that optimum (Pörtner & Peck, 2010):

$$\log\left(N_{s,t}\right) = \alpha_t + \beta_1 T_s + \beta_2 T_s^2 + \varepsilon_N, \quad (1)$$

where the quadratic effect of local temperature, T_s, on the log local density is described by the regression coefficients, β_1 and β_2, while yearly varying intercepts are indicated by the α_t, where t is the year. Residuals, ε_N, represent the local density not accounted for by temperature, and are assumed to be normally distributed with mean zero and variance estimated by the model ('$N\left(0,\sigma^2\right)$').

To estimate the spatial autocorrelation, we then estimated empirical variograms of $\log\left(N_{s,t}\right)$ and ε_N independently. Empirical variograms estimate the average semivariance (i.e. a measure of the average degree of variation between values at distance d) of the data at different distance-bins of separation. Given the parameter of interest ($\log\left(N_{s,t}\right)$ or ε_N, here represented by Z for simplicity) measured at different locations (denoted by subscripts s and x), we estimate its average semivariance at distance, $\gamma(d)$, as:

$$\gamma(d) = \frac{1}{2P(d)} \sum_{P(d)} \left(Z_s - Z_x\right)^2, \quad (2)$$

where P is the number of pairwise observations at distance d. Theoretical variogram models were then fitted to the empirical variogram to describe potential changes in semivariance as a function of distance, which would indicate spatial correlation (Ciannelli et al., 2008). We fitted theoretical variogram models with Gaussian shapes, because they presented the best fit to the empirical variograms of the models tested (exponential, spherical, Gaussian):

$$\gamma(d) = \left(\gamma_\infty - \gamma_0\right) e^{\left(-\frac{d^2}{2R^2}\right)} + \gamma_0 1_{(0,\infty)}(d), \quad (3)$$

where R represents the *range* of the variogram, equals a standard deviation of the Gaussian function and is used as a proxy for the distance of spatial autocorrelation. Changes in semivariance with increasing distance indicate spatial autocorrelation in the data (Ciannelli et al., 2008). The variogram's *range* and *sill* (γ_∞, degree of semivariance among sites separated by distances greater than the range of autocorrelation or constant background variance among sites independent of distance) parameters were optimised using R-package *gstat* (version 2.0-6; Pebesma, 2004). We omitted the *nugget* (γ_0, semivariance at zero distance) from the optimisation processes, restricting it to zero, because it is expected to be influenced by sampling errors and variation on a scale smaller than the sampling resolution, rather than the large-scale thermal effects which we were interested in.

To assess the effect of temperature on the spatial autocorrelation in the density of a species a given year, we measured the relative differences (δ) in the *range* and *sill* of the autocorrelation in density with and without accounting for temperature effects. Using θ to refer to either the *range* or *sill* we get:

13652656, 2023, 11, Downloaded from https://besjournals.onlinelibrary.wiley.com/doi/10.1111/1365-2656.14008 by Institute Of Marine Research, Wiley Online Library on [21/11/2023]. See the Terms and Conditions (https://onlinelibrary.wiley.com/terms-and-conditions) on Wiley Online Library for rules of use; OA articles are governed by the applicable Creative Commons License

$$\delta_\theta = \frac{\theta_{\log(N)} - \theta_{\varepsilon_N}}{\theta_{\log(N)}}, \quad (4)$$

where positive values for δ_θ indicate a positive autocorrelating effect of temperature on density, while negative δ_θ indicate decorrelating effects of temperature on population density. The autocorrelation analyses were restricted to years with a minimum of 15 sites with data since fewer sites resulted in highly uncertain estimates.

2.5 | Local effects on density

We examined spatial patterns in local annual changes in density (r_t), which we estimated by dividing the local density of a given year (N_t) by the density of the previous year (N_{t-1}) and log transforming, $r_t = \log(N_t / N_{t-1})$. We studied the effects that density dependence and temperature had on r_t individually and in combination with each other. Local strength of density dependence was estimated by fitting a Gompertz model (Dennis & Taper, 1994) to each site:

$$r_t = \beta_0 + \beta_1 \log(N_{t-1}) + \varepsilon_t, \quad (5)$$

where β_1 is the strength of local density dependence, β_0 is the model's intercept and $\varepsilon_t \sim N(0, \sigma^2)$ is the residuals or variation in local changes in density unexplained by the estimated density dependence. Increasingly negative β_1 estimates indicate a stronger density dependence. Similarly, we estimated the local effects of temperature on changes in density with:

$$r_t = \beta_0 + \beta_1 T_{t-1} + \varepsilon_t, \quad (6)$$

where $\varepsilon_t \sim N(0, \sigma^2)$ represents the residual variation in r_t unexplained by temperature. We were not able to allow temperature to have a quadratic effect, as we did in the case of yearly spatial autocorrelation, because there were too few points for each site (i.e. number of years with consecutive local density estimates) to generate reliable estimates. Lastly, we assessed how local density dependence and temperature combined predicted changes in density in each site with the following additive model:

$$r_t = \beta_0 + \beta_1 \log(N_{t-1}) + \beta_2 T_{t-1} + \varepsilon_t, \quad (7)$$

where $\varepsilon_t \sim N(0, \sigma^2)$.

2.6 | Spatial synchrony

We estimated the spatial synchrony in annual local changes in density (r) and in the annual local changes in density not predicted by density dependence and/or temperature, that is residuals from Equations 5–7, parametrically (Engen et al., 2005; Grøtan et al., 2005). We used the same approach to estimate the spatial synchrony for each of these variables and will therefore use variable y to represent either of them in the following. Before applying the spatial synchrony models, each variable was locally centred across years, $y = \boldsymbol{y} - \overline{y}$ and then scaled by the standard deviation, that is $\sqrt{\sum(y^2)/(n-1)}$, where y is a vector containing the local annual values of the variable and n is the number of years with data. The spatial synchrony model describes y at site s and time t as

$$y(s,t) = \kappa(s) + W(s,t) + \varepsilon(s,t), \quad (8)$$

where $\kappa(s)$ is the mean at site s, and $W(s,t)$ and $\varepsilon(s,t)$ are the spatially dependent and independent variables, respectively, both with zero means. The spatially dependent variable, $W(s,t)$, represents the spatially structured deviations from $\kappa(s)$, and the spatially independent variable, $\varepsilon(s,t)$, represents the residual variability caused by randomness and sampling error. How the spatially structured variable deviates from the mean with distance (d) is described by the covariance function

$$C_w(d) = Cov(W(s,t), W(b,t)) = \sigma(s)\sigma(b)\rho(d), \quad (9)$$

where covariation between two sites, s and b, is dependent on the variance within each site, and the synchrony, ρ, which depends on the distance (d) separating the sites. The way ρ varies with distance is described as

$$\rho(d) = \rho_\infty + (\rho_0 - \rho_\infty) h(d), \quad (10)$$

where ρ_0 is the degree of synchrony at distances approaching zero, ρ_∞ is the degree of synchrony between points infinitely far apart and $h(d)$ is a Gaussian function, $e^{\left(-\frac{d^2}{2l^2}\right)}$, that describes the rate of decline in synchrony with increasing distance, where l is the standard deviation of the Gaussian function, that is the distance at which around 68% of the drop in synchrony between ρ_0 and ρ_∞ has occurred, and can be used as a spatial scaling measure of spatial autocorrelation (Engen et al., 2005; Lande et al., 1999).

Finally, the values of a variable at time t, $\boldsymbol{y}_t$, can be described by $E(\boldsymbol{y}_t | \boldsymbol{\kappa}) = \boldsymbol{\kappa}$ and $Var(\boldsymbol{y}_t | \boldsymbol{\kappa}) = \boldsymbol{\Sigma} + \sigma_\varepsilon^2 \boldsymbol{I}$, where $\boldsymbol{\Sigma}$ is the spatial covariance and $\sigma_\varepsilon^2 \boldsymbol{I}$ is the spatially independent covariance. Assuming that W and ε are lognormally distributed, the mean corrected values should be multivariate normally distributed, and we can use the likelihood function to estimate ρ_0, ρ_∞ and l. For the optimisation of the likelihood functions used to estimate the synchrony parameters, l was constrained to values between the minimum and maximum distance between sites for each species. Confidence intervals of parameters were estimated through parametric bootstrapping, using the estimated ρ_0, ρ_∞ and l parameters to define multivariate normal distributions from which random values were drawn to refit the model for each bootstrap sample (5000 times per species, resolution, and variable). Lastly, we compared the spatial synchrony in r to the spatial synchrony of local changes in density unexplained by temperature and/or density dependence, that is residuals from Equations 5–7. If synchrony in r is higher than synchrony in residuals from a given model, the variable in that model was assumed to have a synchronizing effect. In contrast, if the residuals were more synchronous, the variable in the model had a desynchronizing effect. All data analyses were carried out using R version 4.1.2 (R Core Team, 2021).

13652656, 2023, 11, Downloaded from https://besjournals.onlinelibrary.wiley.com/doi/10.1111/1365-2656.14008 by Institute Of Marine Research, Wiley Online Library on [21/11/2023]. See the Terms and Conditions (https://onlinelibrary.wiley.com/terms-and-conditions) on Wiley Online Library for rules of use; OA articles are governed by the applicable Creative Commons License

3 | RESULTS

3.1 | Spatial distribution and autocorrelation patterns

Average local SBT varied from 6.21°C in the southwest edge of the sampled area to −1.25°C in the northeast, with an average of 1.71°C and a median of 2.03°C (Figure 1). Most of the study species were caught at least once across most of the study region, with the exceptions of blue whiting and Norway pout, which were absent from the colder eastern Barents Sea, suggesting that the Barents Sea contains the northern edge of their distributions, and herring which was absent in the north (Figure S2). The variogram analyses showed high interannual and interspecific variation in spatial autocorrelation in density (Figure S3). Lumpfish, the least abundant species, showed the shortest average range of autocorrelation and lowest sill (Table 1). In contrast, Norway pout and blue whiting showed the highest sills and long autocorrelation ranges. The range of autocorrelation of long rough dab was similarly long to Norway pout's, but its sill was almost as low as lumpfish's. The other species ranked as follows, from shortest to longest range: herring, capelin, cod, beaked redfish, and haddock (Table 1).

For most species and years, the spatial autocorrelation in density was greater than the autocorrelation in the density residuals after accounting for the effect of temperature, which indicates that the spatial autocorrelation in temperature affected the autocorrelation in population density. On average, temperature explained a larger proportion of the spatial autocorrelation in population density of Norway pout, long rough dab, haddock, followed by beaked redfish, blue whiting, lumpfish and lastly, cod and capelin (Table 1). Temperature was not found to play an important role in the autocorrelation pattern of herring (Table 1; Figure 2). In general, temperature accounted for an increasing proportion of the sill in Norway pout (0.010 (regression coefficient) [0.005, 0.015] (95% confidence intervals)), beaked redfish (0.010 [0.003, 0.017]), lumpfish (0.011 [0.006, 0.016]) and long rough dab (0.008 [0.001, 0.016]), indicating a stronger autocorrelating effect of temperature in later years (Figure 2). Temperature also accounted for an increasing proportion of the range of autocorrelation in the density of Norway pout (0.009 [0.003, 0.015]) and long rough dab (0.010 [0.003, 0.017]).

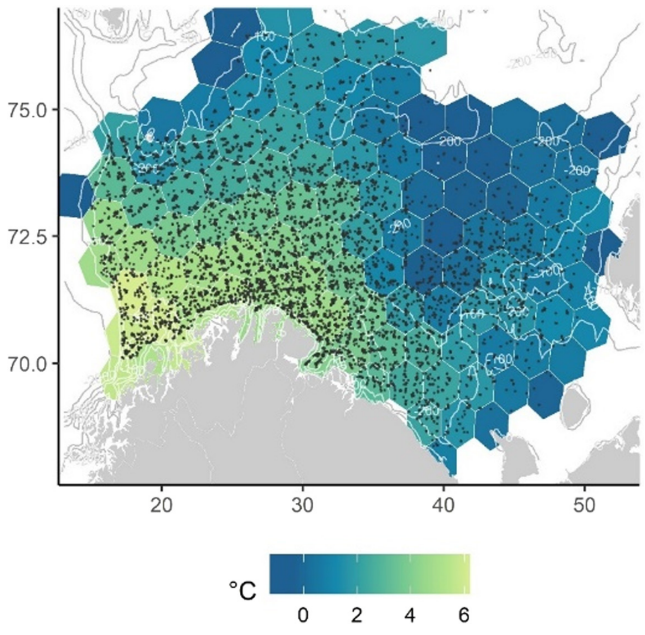

FIGURE 1 Map of the Barents Sea overlaid with the hexagonal grid used to define each site. The grid colours indicate the average site's sea bottom temperature (SBT) recorded during the survey, 1986–2015, January–March. Each dot represents a trawl. The larger grey areas represent land masses and the depth profile is indicated by bathymetry lines.

3.2 | Local effects of temperature and density dependence

Spatial patterns in the effects of density dependence and temperature on local density dynamics varied among species (Figure 3). The effects of temperature on density dynamics showed a clearer spatial structure when examined in combination with the effects of density dependence (Figure 3), than without (Figure S4). The local strength of density dependence was on average weakest in Norway pout and blue whiting, the two species with the greatest affinity for warm waters. Local strength of density dependence was most spatially clustered in beaked redfish, haddock, cod and long rough dab, resulting in large patches with strong density dependence and large patches of weak or no density dependence. Capelin, lumpfish and herring also showed some spatial variation in the strength of density dependence, but they were strongly density-dependent across a larger extent of their studied ranges compared to the other species.

The local effects of temperature on density were positive across most of the range of Norway pout and blue whiting (Figure 3). The southwestern Barents Sea represents the north-easternmost boundary of Norway pout's and blue whiting's distributions, and temperature is expected to have a stronger effect on abundance around the latitudinal boundaries of a species distributions, as these are often related to thermal tolerance (Heino et al., 2008; Husson et al., 2020). In beaked redfish, haddock, cod and long rough dab, warming had positive effects largely limited to the east, possibly influenced by the strong thermal gradient of the Polar front (i.e. where warm Atlantic waters meet cold Arctic waters; Husson et al., 2020). In addition, warming had weak negative effects along the southwestern distribution margin in beaked redfish, cod, and lumpfish. The response of capelin to warming differed from the other species, where negative correlations with temperature predominated in the north of their distributions and positive in the south. Lastly, the effect of temperature on herring was highly heterogeneous.

3.3 | Spatial synchrony

The scaling of spatial synchrony, *I*, (i.e. a standard deviation of the Gaussian function describing the change in synchrony with

13652656, 2023, 11, Downloaded from https://besjournals.onlinelibrary.wiley.com/doi/10.1111/1365-2656.14008 by Institute Of Marine Research, Wiley Online Library on [21/11/2023]. See the Terms and Conditions (https://onlinelibrary.wiley.com/terms-and-conditions) on Wiley Online Library for rules of use; OA articles are governed by the applicable Creative Commons License

Species	$\log(N_t)$		δ	
	Range (km)	Sill	Range	Sill
Norway pout	155 (97–254)	6.69 (2.83–10.65)	0.42	0.64
Blue whiting	137 (69–393)	5.58 (2.16–15.33)	0.08	0.11
Beaked redfish	116 (65–255)	3.42 (2.07–5.4)	0.10	0.20
Haddock	126 (73–250)	3.02 (1.17–8.41)	0.22	0.39
Cod	108 (52–176)	1.04 (0.39–4.71)	0.05	0.08
Capelin	105 (50–178)	4.38 (2.39–7.65)	0.04	0.08
Lumpfish	96 (31–160)	0.83 (0.43–1.4)	0.06	0.11
Long rough dab	143 (109–354)	1.21 (0.78–2.54)	0.32	0.42
Herring	97 (53–313)	3.35 (1.25–10.45)	−0.01	0.01

Note: In brackets are the values for the years with the minimum and maximum estimates. Darker green is indicative of greater parameter values relative to the other species. On the right, relative proportion of the spatial autocorrelation associated to the direct effect of sea bottom temperature (δ in Equation 4), where darker red indicates a greater proportion of autocorrelation related to temperature.

TABLE 1 Medians of the ranges and sills (i.e. semivariance between sites separated by distances greater than the estimated range of autocorrelation, or constant background variance among sites independent of distance) of the variograms estimating the annual spatial autocorrelation in density, that is $\log(N_t)$, between 1985 and 2016.

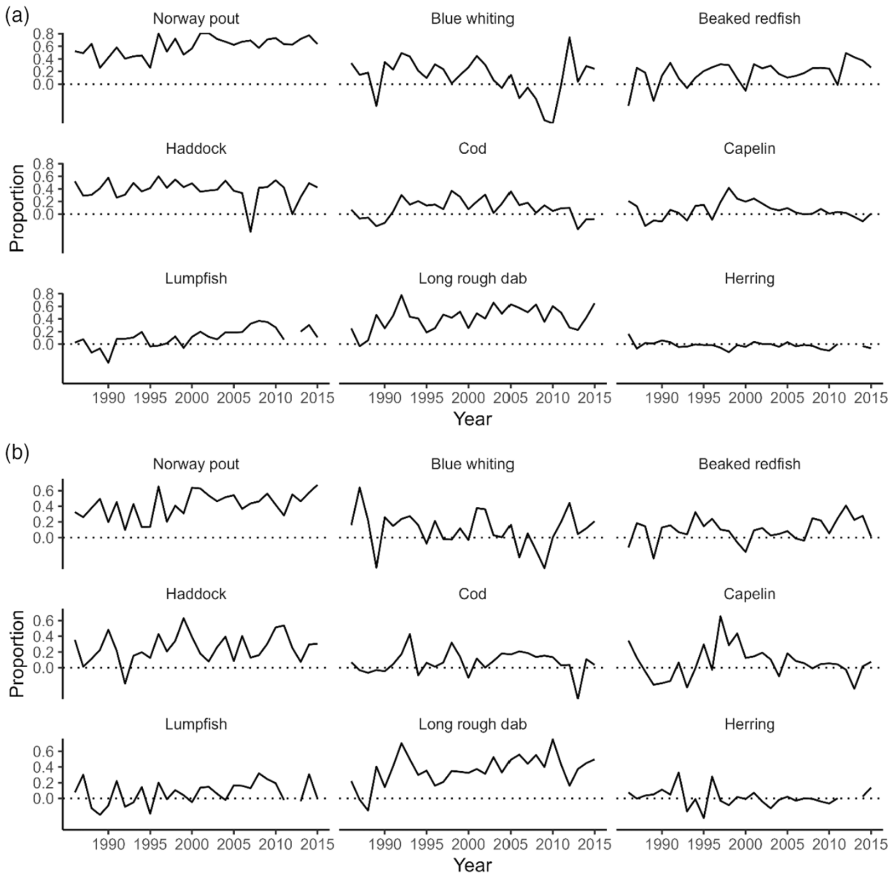

FIGURE 2 Black lines show the relative proportion of the sill (a) and range (b) of the spatial autocorrelation in the density of each species and year that is explained by temperature (i.e. δ_θ in Equation 4). In 2012 for lumpfish, and 2011 to 2013 for herring, less than 15 sites had matching records of species occurrences and temperature, which was below the threshold of minimum amount of data that we had established to estimate reliable autocorrelation estimates.

increasing distance, see Gaussian function within Equation 10) in local changes in density (r) was shortest in capelin followed by haddock, and lumpfish (Table 2; Figure 4). At the other end of the scale, spatial synchrony in changes in density showed the longest scaling in cod and long rough dab. They were followed closely by blue whiting, which had one of the smallest distributional range coverages within the study area and showed the overall highest degree of synchrony. Norway pout, herring and beaked redfish showed intermediate spatial scaling. After blue whiting, the degree of synchrony in changes in density at distances approaching zero was highest in haddock, Norway pout, herring and cod. In contrast, long rough dab, beaked redfish and lumpfish showed very little synchrony at short distances. Besides blue whiting, Norway pout, haddock and long rough dab, the synchrony in local changes in density at very long distances was below 0.1 for all species.

Because there was a high degree of overlap between the confidence intervals of the synchrony in the annual density variation and the synchrony in the model residuals (Figure S5), we focus on results

13652656, 2023, 11, Downloaded from https://besjournals.onlinelibrary.wiley.com/doi/10.1111/1365-2656.14008 by Institute Of Marine Research, Wiley Online Library on [21/11/2023]. See the Terms and Conditions (https://onlinelibrary.wiley.com/terms-and-conditions) on Wiley Online Library for rules of use; OA articles are governed by the applicable Creative Commons License

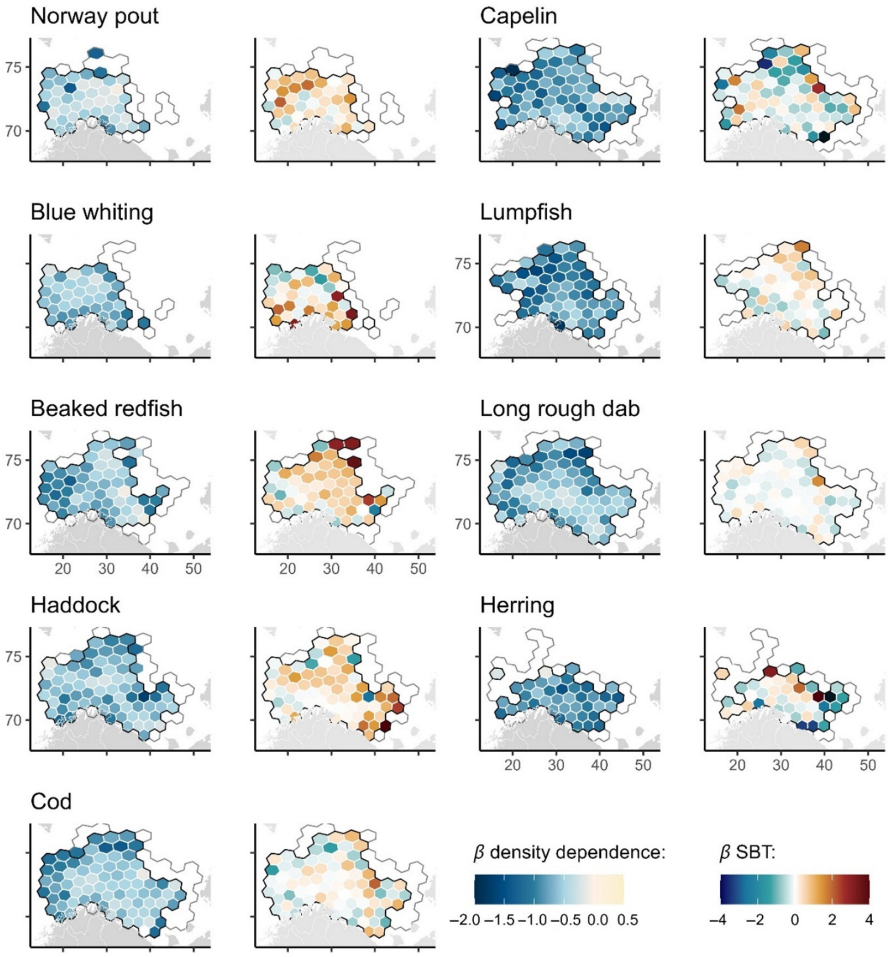

FIGURE 3 Maps of the Barents Sea with the hexagonal grid used to define each site. The colours represent the regression coefficient (β) of the variables used to estimate species-specific annual local changes in density, that is density dependence and sea bottom temperature (SBT), when modelling changes in density with both variables together in the model. Lower (or more negative) regression coefficients in the density dependence represent stronger density dependence. The outer grey polygon represents the sites in which the species have been caught at least once, however, only sites with more than five data points were included (black inner polygon).

that were consistent across species or which showed least overlapping confidence intervals. Overall, local density dependence tended to have a desynchronizing effect on the local annual changes in density at distances approaching zero for most species, with the desynchronizing effect being most noticeable in cod, herring, long rough dab, beaked redfish, capelin and Norway pout (Table 2). Density dependence also showed a desynchronizing effect on changes in density at very long distances in Norway pout and cod, as well as capelin and haddock to a lesser extent, and little to no effect in the other species. Despite the overall desynchronizing effect of density dependence, it had a positive effect on the scale of synchrony in cod, herring and Norway pout, and negative effect in beaked redfish. No effect of density dependence on the synchrony in changes in density of blue whiting was found.

In contrast to density dependence, temperature tended to synchronise annual changes in density, as shown by the generally lower degree of synchrony in the residuals of the model accounting for temperature, although, the synchronizing effect of temperature was minimal (Table 2) in some species (capelin, lumpfish, herring; Figure 4). The synchronizing effect of temperature was highest in beaked redfish and blue whiting, followed by long rough dab and haddock. There was no clear effect of temperature on the scale of synchrony in changes in density across all species. Still, temperature had a negative effect on the scale of synchrony in blue whiting, long rough dab, and Norway pout.

Because the temperature and density dependence generally had contrasting effect on spatial synchrony, that is temperature synchronised and density dependence desynchronised, they tended to cancel each other out resulting in spatial synchrony in the residual changes in density that very closely resembled the synchrony pattern of the raw annual changes in density. Still, the stronger desynchronizing effect of density dependence compared to the synchronizing effect of temperature at short distances was evident in most species: long rough dab, beaked redfish, capelin, cod, herring and Norway pout (Table 2).

4 | DISCUSSION

We provide empirical evidence showing that the annual local changes in density of fish in the Barents Sea tend to be spatially synchronised by temperature, and spatially desynchronised by local density dependence (Figure 4). While the effects of these variables on the spatial synchrony of changes in density were weak in most species, they were consistent across all our study species. Species whose presence in the Barents Sea are mostly associated with the leading edge of their distribution were more synchronised by temperature than more northern species whose ranges were already well established across the entire Barents

13652656, 2023, 11, Downloaded from https://besjournals.onlinelibrary.wiley.com/doi/10.1111/1365-2656.14008 by Institute Of Marine Research, Wiley Online Library on [21/11/2023]. See the Terms and Conditions (https://onlinelibrary.wiley.com/terms-and-conditions) on Wiley Online Library for rules of use; OA articles are governed by the applicable Creative Commons License

TABLE 2 Median and 95% confidence intervals of the parameters in the bootstrapped spatial synchrony models estimating synchrony in change in density (left side), where *l* is the scale of synchrony, ρ_0 is the degree of synchrony at distances approaching zero and ρ_∞ is the synchrony at infinity (Equation 10).

Species	Synchrony in changes in density			Absolute effect of variables on the synchrony parameter									
				l (km)			ρ_0			ρ_∞			
	l (km)	ρ_0	ρ_∞	T	D	$T+D$	T	D	$T+D$	T	D	$T+D$
Norway pout	181 (90–483)	0.43 (0.33–0.56)	0.20 (0.00–0.35)	76.75	−50.01	−60.50	−0.04	0.05	0.04	−0.07	0.08	0.06
Blue whiting	188 (125–305)	0.64 (0.57–0.72)	0.22 (0.00–0.40)	30.21	12.23	27.49	−0.03	0.01	−0.01	−0.15	0.00	−0.05
Beaked redfish	186 (98–340)	0.30 (0.22–0.39)	0.06 (0.00–0.17)	−23.76	36.53	−4.62	−0.05	0.05	0.03	−0.05	−0.01	0.01
Haddock	121 (90–165)	0.49 (0.41–0.57)	0.20 (0.12–0.27)	−0.57	1.89	−4.14	−0.02	0.03	−0.02	−0.03	0.04	−0.02
Cod	216 (132–290)	0.42 (0.36–0.49)	0.06 (0.00–0.18)	−3.55	−35.88	−14.36	−0.02	0.08	0.03	−0.02	0.05	0.06
Capelin	108 (90–150)	0.38 (0.27–0.48)	0.00 (0.00–0.06)	−2.44	11.41	−1.70	−0.03	0.05	0.04	0.00	0.03	0.05
Lumpfish	124 (90–229)	0.32 (0.19–0.48)	0.03 (0.00–0.16)	7.07	10.69	12.82	−0.02	0.03	0.00	0.00	−0.02	−0.01
Long rough dab	192 (102–408)	0.28 (0.21–0.37)	0.13 (0.00–0.21)	31.59	−19.52	−38.47	−0.02	0.05	0.06	−0.03	−0.02	0.01
Herring	186 (90–355)	0.42 (0.31–0.60)	0.08 (0.00–0.26)	−38.79	−53.24	−52.33	0.00	0.08	0.08	−0.01	−0.03	−0.03

Note: Darker shade indicates a higher parameter value relative to the other species. On the right side, changes in the parameter after accounting for the effect of local temperature (*T*), local density dependence (*D*) and their additive effect (*T*+*D*) on changes in density. Red indicates synchronizing effect by the variable, blue indicates desynchronizing effect, and the shade shows the strength of the effect, where darker is stronger.

Sea. Our results agree with theoretical studies predicting a negative effect of strong density dependence on spatial synchrony (Engen & Sæther, 2005; Lande et al., 1999), and empirical studies highlighting the important roles that density dependence and environmental conditions, such as temperature, can play in driving spatial synchrony in wild populations (Hansen et al., 2020; Herfindal et al., 2020; Myers et al., 1997; Nicolau et al., 2022; Post & Forchhammer, 2004; Sæther et al., 2007).

Temperature can strongly influence the spatial (Husson et al., 2020) and temporal (Dingsør et al., 2007) variation in the dynamics of populations (Ottersen & Loeng, 2000; Poloczanska et al., 2016). Here, the observed scaling of spatial synchrony in annual changes in density was similar to the scaling of synchrony in sea temperature estimated in other studies (Herfindal et al., 2022), suggesting that sea temperature generates spatial synchrony in population fluctuations. In addition, when analysing the spatial density distribution of individual years, temperature was shown to be an important factor autocorrelating the distribution of species like Norway pout and long rough dab, possibly through its regulation of local carrying capacities and habitat suitability (Figure 2; Myers, 2001). However, we found that, while local temperature had a synchronizing effect on the density dynamics of most Barents Sea fish, this synchronizing effect was weak. The species whose synchrony was most influenced by temperature were those with the strongest association to warmer waters within the Barents Sea, that is blue whiting, haddock, beaked redfish, and Norway pout. The synchronizing effect of temperature on these species was probably further influenced by the fact that our data was collected during winter, and colder winter temperatures pose a stronger regulation on the vital rates of more southern species, who find themselves closer to their thermal tolerance limits. The strong synchronizing effect of temperature on the northward distributional edge of southern species within the Barents Sea highlights the high vulnerability of these populations to declines in temperature. Similarly, warm years could induce synchronous increases in density across large areas. As densities of southern species increase synchronously across large extents, their probability of successful establishment in the regions increases since local predators are less capable of down regulating their densities (Bjørnstad et al., 2008), also leading to greater instability in the system (Liu et al., 2016).

Density dependence was found to spatially desynchronise local fluctuations in population density in most of the studied species, particularly over shorter distances. Theory predicts that populations with stronger density dependence will tend to return faster toward a carrying capacity (Lande et al., 1999). At local scales, this implies that in populations with strong density dependence, departures from the local carrying capacity are offset faster locally, preventing local changes in density from influencing other locations through dispersal, thereby desynchronizing density (Engen & Sæther, 2005; Marquez et al., 2019). We did not find a clear relationship between the distribution of local strengths of density dependence (Figure 3) and the effects of that local density dependence on synchrony

13652656, 2023, 11, Downloaded from https://besjournals.onlinelibrary.wiley.com/doi/10.1111/1365-2656.14008 by Institute Of Marine Research, Wiley Online Library on [21/11/2023]. See the Terms and Conditions (https://onlinelibrary.wiley.com/terms-and-conditions) on Wiley Online Library for rules of use; OA articles are governed by the applicable Creative Commons License

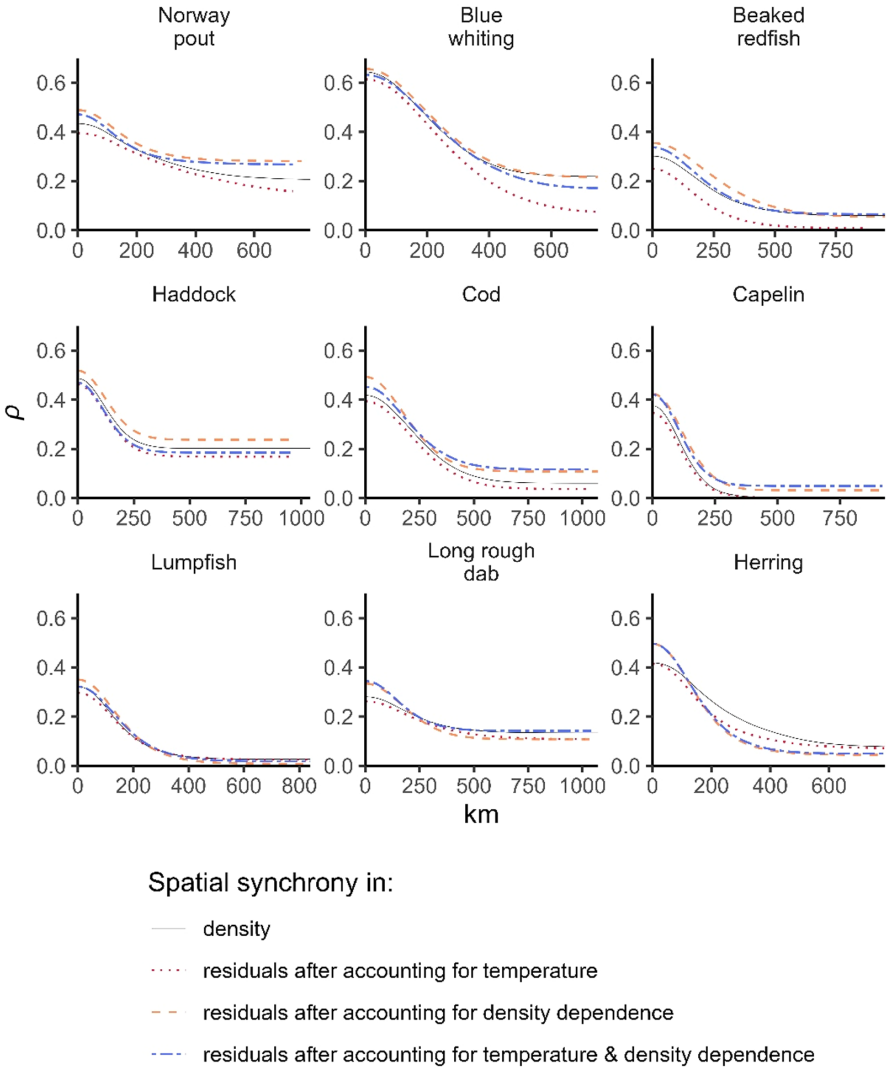

FIGURE 4 Spatial synchrony in annual changes in density (i.e. not accounting for the effects of any other variables) and its residuals after accounting for the effects of temperature, density dependence and both together. Each plot is representative of the dynamics of the species indicated over the plot.

(Table 2). It is possible that the Gompertz model used here to provide rough approximations of the density-dependent dynamics was useful for identifying regions of stronger or weaker density dependence but insufficient to provide accurate measurements of the expected changes in density. Changes in density could follow more complex nonlinear dynamics influenced by, for example, changes in interspecific interactions and age structure (Marquez et al., 2021). More advanced multi-species population models might therefore present great potential for future research aiming to disentangle the effects of density dependence on spatial synchrony in population fluctuations.

This study focused on the direct effects of temperature and density dependence, but these two variables are also likely to have time-lagged and non-local effects on density dynamics, and thereby on synchrony, which might be more difficult to disentangle. For example, density dependence and temperature are known to have strong effects on recruitment rates and year-class strength, that is cohort size at the end of the larval stage (Dingsør et al., 2007), and strong year-classes have been shown to remain large in subsequent years (Myers, 2001; Ottersen & Loeng, 2000). Population density dynamics could therefore be spatially synchronised by large cohorts produced by good years, which disperse and settle homogenously as they age (Planque et al., 2011). The demographic structure of the population can also influence how spatial synchrony in density is affected by local density dependence and temperature (Marquez et al., 2021). For instance, older and larger individuals within a population are likely to be less sensitive to adverse environmental impacts than smaller individuals. As such, if the population is spatially age-segregated (Bogstad et al., 1994), environmental effects might be felt more in regions dominated by younger individuals. Similarly, years when the population age structure is skewed toward younger age class might be more sensitive to environmental factors than years when the average age in the population is higher. Future empirical studies should explore the effects of harvesting on synchrony, since harvesting is known to influence the structures and dynamics of populations, thus affecting synchrony (Jarillo et al., 2018). Lastly, while density dependence was found to be very weak in blue whiting, previous studies have highlighted that blue whiting abundance in the Barents Sea is highly influenced by density-dependent spillover from the main population located along the Norwegian Sea (Heino et al., 2008).

13652656, 2023, 11, Downloaded from https://besjournals.onlinelibrary.wiley.com/doi/10.1111/1365-2656.14008 by Institute Of Marine Research, Wiley Online Library on [21/11/2023]. See the Terms and Conditions (https://onlinelibrary.wiley.com/terms-and-conditions) on Wiley Online Library for rules of use; OA articles are governed by the applicable Creative Commons License

The results presented here highlight the complexity of potential drivers of spatial synchrony in population dynamics. We show that, while temperature regulates local changes in density and patterns of spatial autocorrelation in the distribution of several marine fish populations, its effects on spatial synchrony were weak. The positive effect of temperature on spatial synchrony was nevertheless stronger among the species with more southern affinities expanding their ranges into the Barents Sea. This has important implications for conservation, as it confirms that species should become increasingly synchronised as they shift their ranges to track their thermal optima globally, especially those species that do not manage to shift range at the same rate as the climate around them (Poloczanska et al., 2013). Similarly, the desynchronizing effect of density dependence was not uniform across species, possibly because of complex and heterogeneous interspecific interactions (Lee et al., 2020).

Spatial population synchrony influences crucial ecological processes and management decisions, including vulnerability to diseases outbreaks (Bjørnstad, 2000; Viboud et al., 2006), harvesting (Jarillo et al., 2020), and ultimately extinction risk (Heino et al., 1997). No single process is likely to be solely responsible for the spatial synchrony exhibited by a species. Therefore, quantifying the relative effects of potential synchronizing and desynchronizing forces provides a good approach to understanding synchrony. Considering the environmental changes projected for the Barents Sea (Johannesen et al., 2012) and globally, improving our understanding of individual synchrony drivers is essential for achieving sustainable conservation and management goals (Hansen et al., 2020).

AUTHOR CONTRIBUTIONS

Bernt-Erik Sæther, Aline Magdalena Leeand Jonatan F. Marquez planned the study. Sondre Aanesand Are Salthaugcollected the data. Jonatan F. Marquez performed all statistical analyses with input from Sondre Aaneson the code and input from Bernt-Erik Sæther, Ivar Herfindaland Aline Magdalena Leeon the statistical approach. Jonatan F. Marquez wrote the manuscript with contributions from all authors.

ACKNOWLEDGEMENTS

We thank the people in the Russian Polar Research Institute of Marine Fisheries and Oceanography and the Norwegian Institute of Marine Research for collecting the data used in our research. This study was funded by the Research Council of Norway through the Centre of Excellence Centre for Biodiversity Dynamics (project no. 223257) and to the project 'Sustainable management of renewable resources in a changing environment: an integrated approach across ecosystems' (SUSTAIN) (project no. 244647). Lastly, we thank the editors and reviewers for the comments and suggestions for improving this paper.

CONFLICT OF INTEREST STATEMENT

The authors have no conflicts of interest to declare.

DATA AVAILABILITY STATEMENT

Data available from the Dryad Digital Repository https://doi.org/10.5061/dryad.g79cnp5w2 (Marquez & Aanes, 2023).

ORCID

Jonatan F. Marquez https://orcid.org/0000-0003-2034-6634
Ivar Herfindal https://orcid.org/0000-0002-5860-9252
Bernt-Erik Sæther https://orcid.org/0000-0002-0049-9767
Aline Magdalena Lee https://orcid.org/0000-0001-9272-4249

REFERENCES

Aune, M., Aschan, M. M., Greenacre, M., Dolgov, A. V., Fossheim, M., & Primicerio, R. (2018). Functional roles and redundancy of demersal Barents Sea fish: Ecological implications of environmental change. *PLoS ONE*, *13*(11), 1–21. https://doi.org/10.1371/journal.pone.0207451

Bjørnstad, O. N. (2000). Cycles and synchrony: Two historical 'experiments' and one experience. *Journal of Animal Ecology*, *69*(5), 869–873. https://doi.org/10.1046/j.1365-2656.2000.00444.x

Bjørnstad, O. N., Ims, R. A., & Lambin, X. (1999). Spatial population dynamics: Analyzing patterns and processes of population synchrony. *Trends in Ecology & Evolution*, *14*(11), 427–432. https://doi.org/10.1016/S0169-5347(99)01677-8

Bjørnstad, O. N., Liebhold, A. M., & Johnson, D. M. (2008). Transient synchronization following invasion: Revisiting Moran's model and a case study. *Population Ecology*, *50*(4), 379–389. https://doi.org/10.1007/s10144-008-0105-5

Bogstad, B., Lilly, G. R., Mehl, S., Pálsson, Ó., & Stefánsson, G. (1994). Cannibalism and year-class strength in Atlantic cod (*Gadus morhua* L.) in Arcto-boreal ecosystems (Barents Sea, Iceland, and eastern Newfoundland). *ICES Marine Science Symposia*, *198*, 576–599.

Cheal, A. J., Delean, S., Sweatman, H., & Thompson, A. A. (2007). Spatial synchrony in coral reef fish populations and the influence of climate. *Ecology*, *88*(1), 158–169. https://doi.org/10.1890/0012-9658(2007)88[158:SSICRF]2.0.CO;2

Ciannelli, L., Fauchald, P., Chan, K. S., Agostini, V. N., & Dingsør, G. E. (2008). Spatial fisheries ecology: Recent progress and future prospects. *Journal of Marine Systems*, *71*(3–4), 223–236. https://doi.org/10.1016/j.jmarsys.2007.02.031

Dalpadado, P., Ingvaldsen, R. B., Stige, L. C., Bogstad, B., Knutsen, T., Ottersen, G., & Ellertsen, B. (2012). Climate effects on Barents Sea ecosystem dynamics. *ICES Journal of Marine Science*, *69*(7), 1303–1316. https://doi.org/10.1093/icesjms/fss063

Dennis, B., & Taper, M. L. (1994). Density dependence in time series observations of natural populations: Estimation and testing. *Ecological Monographs*, *64*(2), 205–224. https://doi.org/10.2307/2937041

Dingsør, G. E., Ciannelli, L., Chan, K. S., Ottersen, G., & Stenseth, N. C. (2007). Density dependence and density independence during the early life stages of four marine fish stocks. *Ecology*, *88*(3), 625–634. https://doi.org/10.1890/05-1782

Engen, S. (2017). Spatial synchrony and harvesting in fluctuating populations: Relaxing the small noise assumption. *Theoretical Population Biology*, *116*, 18–26. https://doi.org/10.1016/j.tpb.2017.06.002

Engen, S., Lande, R., & Sæther, B.-E. (2002). The spatial scale of population fluctuations and quasi-extinction risk. *The American Naturalist*, *160*(4), 439–451. https://doi.org/10.1086/342072

Engen, S., Lande, R., Sæther, B.-E., & Bregnballe, T. (2005). Estimating the pattern of synchrony in fluctuating populations. *Journal of Animal Ecology*, *74*(4), 601–611. https://doi.org/10.1111/j.1365-2656.2005.00942.x

13652656, 2023, 11, Downloaded from https://besjournals.onlinelibrary.wiley.com/doi/10.1111/1365-2656.14008 by Institute Of Marine Research, Wiley Online Library on [21/11/2023]. See the Terms and Conditions (https://onlinelibrary.wiley.com/terms-and-conditions) on Wiley Online Library for rules of use; OA articles are governed by the applicable Creative Commons License

Engen, S., & Sæther, B.-E. (2005). Generalizations of the Moran effect explaining spatial synchrony in population fluctuations. *The American Naturalist*, *166*(5), 603–612. https://doi.org/10.1086/491690

Eriksen, E., Benzik, A. N., Dolgov, A. V., Skjoldal, H. R., Vihtakari, M., Johannesen, E., Prokhorova, T. A., Keulder-Stenevik, F., Prokopchuk, I., & Strand, E. (2020). Diet and trophic structure of fishes in the Barents Sea: The Norwegian-Russian program 'year of stomachs' 2015—Establishing a baseline. *Progress in Oceanography*, *183*(December 2019), 102262. https://doi.org/10.1016/j.pocean.2019.102262

Fall, J., de Lange Wenneck, T., Bogstad, B., Fuglebakk, E., Gjøsæter, H., Seim, S. E., Skage, M. L., Staby, A., Tranang, C. A., Windsland, K., Russkikh, A. A., & Fomin, K. (2020). *Fish investigations in the Barents Sea winter 2020*. IMR/PINRO Joint Report Series.

Fay, R., Michler, S., Laesser, J., Jeanmonod, J., & Schaub, M. (2020). Large-scale vole population synchrony in Central Europe revealed by kestrel breeding performance. *Frontiers in Ecology and Evolution*, *7*(January), 1–6. https://doi.org/10.3389/fevo.2019.00512

Fogarty, M. J., & Botsford, L. W. (2007). Population connectivity and spatial management of marine fisheries. *Oceanography*, *20*(SPL.ISS. 3), 112–123. https://doi.org/10.5670/oceanog.2007.34

Fossheim, M., Primicerio, R., Johannesen, E., Ingvaldsen, R. B., Aschan, M. M., & Dolgov, A. V. (2015). Recent warming leads to a rapid borealization of fish communities in the Arctic. *Nature Climate Change*, *5*(May), 1–6. https://doi.org/10.1038/nclimate2647

Fromentin, J.-M., Myers, R. A., Bjørnstad, O. N., Stenseth, N. C., Gjøsæter, J., & Christie, H. (2001). Effects of density-dependent and stochastic processes on the regulation of cod populations. *Ecology*, *82*(2), 567–579. https://doi.org/10.1890/0012-9658(2001)082[0567:EODDAS]2.0.CO;2

Grøtan, V., Sæther, B.-E., Engen, S., Solberg, E. J., Linnell, J. D., Andersen, R., Broseth, H., & Lund, E. (2005). Climate causes large-scale spatial synchrony in population fluctuations of a temperature herbivore. *Ecology*, *86*(6), 1472–1482. https://doi.org/10.1890/04-1502

Hansen, B. B., Grøtan, V., Herfindal, I., & Lee, A. M. (2020). The Moran effect revisited: Spatial population synchrony under global warming. *Ecography*, *43*, 1591–1602. https://doi.org/10.1111/ecog.04962

Heino, M., Engelhard, G. H., & Godø, O. R. (2008). Migrations and hydrography determine the abundance fluctuations of blue whiting (*Micromesistius poutassou*) in the Barents Sea. *Fisheries Oceanography*, *17*(2), 153–163. https://doi.org/10.1111/j.1365-2419.2008.00472.x

Heino, M., Kaitala, V., Ranta, E., & Lindström, J. (1997). Synchronous dynamics and rates of extinction in spatially structured populations. *Proceedings of the Royal Society of London B: Biological Sciences*, *264*(1381), 481–486. https://doi.org/10.1098/rspb.1997.0069

Herfindal, I., Aanes, S., Benestad, R., Finstad, A., Salthaug, A., Stenseth, N., & Sæther, B. (2022). Spatiotemporal variation in climatic conditions across ecosystems. *Climate Research*, *86*, 9–19. https://doi.org/10.3354/cr01641

Herfindal, I., Tveraa, T., Stien, A., Solberg, E. J., & Grøtan, V. (2020). When does weather synchronize life-history traits? Spatiotemporal patterns in juvenile body mass of two ungulates. *Journal of Animal Ecology*, *89*(6), 1419–1432. https://doi.org/10.1111/1365-2656.13192

Hugueny, B. (2006). Spatial synchrony in population fluctuations: Extending the Moran theorem to cope with spatially heterogeneous dynamics. *Oikos*, *115*(1), 3–14. https://doi.org/10.1111/j.2006.0030-1299.14686.x

Huse, G., Railsback, S., & Fernö, A. (2002). Modelling changes in migration pattern of herring: Collective behaviour and numerical domination. *Journal of Fish Biology*, *60*(3), 571–582. https://doi.org/10.1006/jfbi.2002.1874

Husson, B., Certain, G., Filin, A., & Planque, B. (2020). Suitable habitats of fish species in the Barents Sea. *Fisheries Oceanography*, *29*(6), 526–540. https://doi.org/10.1111/fog.12493

Ims, R. A., & Andreassen, H. P. (2000). Spatial synchronization of vole population dynamics by predatory birds. *Nature*, *408*(6809), 194–196. https://doi.org/10.1038/35041562

Jakobsen, T., Korsbrekke, K., Mehl, S., & Nakken, O. (1997). Norwegian combined acoustic and bottom trawl surveys for demersal fish in the Barents Sea during winter. *ICES*, *17*, 26.

Jarillo, J., Sæther, B. E., Engen, S., & Cao, F. J. (2018). Spatial scales of population synchrony of two competing species: Effects of harvesting and strength of competition. *Oikos*, *127*(10), 1459–1470. https://doi.org/10.1111/oik.05069

Jarillo, J., Sæther, B.-E., Engen, S., & Cao-García, F. J. (2020). Spatial scales of population synchrony in predator-prey systems. *The American Naturalist*, *195*(2), 216–230. https://doi.org/10.1086/706913

Johannesen, E., Ingvaldsen, R. B., Bogstad, B., Dalpadado, P., Eriksen, E., Gjøsæter, H., Knutsen, T., Skern-Mauritzen, M., & Stiansen, J. E. (2012). Changes in Barents Sea ecosystem state, 1970–2009: Climate fluctuations, human impact, and trophic interactions. *ICES Journal of Marine Science*, *69*(5), 880–889. https://doi.org/10.1093/icesjms/fss046

Johnson, D. W. (2006). Predation, habitat complexity, and variation in density-dependent mortality of temperate reef fishes. *Ecology*, *87*(5), 1179–1188. https://doi.org/10.1890/0012-9658(2006)87[1179:PHCAVI]2.0.CO;2

Kleisner, K. M., Walter, J. F., Diamond, S. L., & Die, D. J. (2010). Modeling the spatial autocorrelation of pelagic fish abundance. *Marine Ecology Progress Series*, *411*(July), 203–213. https://doi.org/10.3354/meps08667

Lande, R., Engen, S., & Sæther, B.-E. (1999). Spatial scale of population synchrony: Environmental correlation versus dispersal and density regulation. *The American Naturalist*, *154*(3), 271–281. https://doi.org/10.1086/303240

Laurel, B. J., Stoner, A. W., & Hurst, T. P. (2007). Density-dependent habitat selection in marine flatfish: The dynamic role of ontogeny and temperature. *Marine Ecology Progress Series*, *338*, 183–192. https://doi.org/10.3354/meps338183

Lee, A. M., Sæther, B.-E., & Engen, S. (2020). Spatial covariation of competing species in a fluctuating environment. *Ecology*, *101*(1), 1–9. https://doi.org/10.1002/ecy.2901

Liebhold, A. M., Haynes, K. J., & Bjørnstad, O. N. (2012). Spatial synchrony of insect outbreaks. In P. Barbosa, D. K. Letourneau, & A. A. Agrawal (Eds.), *Insect outbreaks revisited* (pp. 113–125). John Wiley & Sons, Ltd. https://doi.org/10.1002/9781118295205.ch6

Liebhold, A. M., Koenig, W. D., & Bjørnstad, O. N. (2004). Spatial synchrony in population dynamics. *Annual Review of Ecology, Evolution, and Systematics*, *35*(1), 467–490. https://doi.org/10.1146/annurev.ecolsys.34.011802.132516

Liu, Z., Zhang, F., & Hui, C. (2016). Density-dependent dispersal complicates spatial synchrony in tri-trophic food chains. *Population Ecology*, *58*(1), 223–230. https://doi.org/10.1007/s10144-015-0515-0

Marquez, J. F., & Aanes, S. (2023). Effects of local density dependence and temperature on the spatial synchrony of marine fish populations. [Dataset]. *Dryad Digital Repository*, https://doi.org/10.5061/dryad.g79cnp5w2

Marquez, J. F., Lee, A. M., Aanes, S., Engen, S., Herfindal, I., Salthaug, A., & Sæther, B.-E. (2019). Spatial scaling of population synchrony in marine fish depends on their life history. *Ecology Letters*, *22*(11), 1787–1796. https://doi.org/10.1111/ele.13360

Marquez, J. F., Sæther, B., Aanes, S., Engen, S., Salthaug, A., & Lee, A. M. (2021). Age-dependent patterns of spatial autocorrelation in fish populations. *Ecology*, *102*, e03523. https://doi.org/10.1002/ecy.3523

13652656, 2023, 11, Downloaded from https://besjournals.onlinelibrary.wiley.com/doi/10.1111/1365-2656.14008 by Institute Of Marine Research, Wiley Online Library on [21/11/2023]. See the Terms and Conditions (https://onlinelibrary.wiley.com/terms-and-conditions) on Wiley Online Library for rules of use; OA articles are governed by the applicable Creative Commons License

May, R. M. (1974). *Stability and complexity in model ecosystems* (Vol. *1*). Princeton University Press. https://doi.org/10.2307/j.ctvs32rq4

May, R. M. (1987). Chaos and the dynamics of biological populations. *Proceedings of the Royal Society of London A. Mathematical and Physical Sciences*, *413*(1844), 27–44. https://doi.org/10.1098/rspa.1987.0098

Mjanger, H., Svendsen, B. V., Senneset, H., Fuglebakk, E., Skage, M. L., Diaz, J., Johansen, G. O., & Vollen, T. (2020). *Handbook for sampling fish, crustaceans and other invertebrates* (Issue November 2019). Marine Research Institute.

Moran, P. (1953). The statistical analysis of the Canadian lynx cycle. II. Synchronization and meteorology. *Australian Journal of Zoology*, *1*(3), 291–298. https://doi.org/10.1071/ZO9530291

Morrongiello, J. R., Horn, P. L., Maolagáin, C. Ó., & Sutton, P. J. H. (2021). Synergistic effects of harvest and climate drive synchronous somatic growth within key New Zealand fisheries. *Global Change Biology*, *27*(7), 1470–1484. https://doi.org/10.1111/gcb.15490

Muffler, L., Weigel, R., Hacket-Pain, A. J., Klisz, M., van der Maaten, E., Wilmking, M., Kreyling, J., & van der Maaten-Theunissen, M. (2020). Lowest drought sensitivity and decreasing growth synchrony towards the dry distribution margin of European beech. *Journal of Biogeography*, *47*(9), 1910–1921. https://doi.org/10.1111/jbi.13884

Myers, J. T., Yule, D. L., Jones, M. L., Ahrenstorff, T. D., Hrabik, T. R., Claramunt, R. M., Ebener, M. P., & Berglund, E. K. (2015). Spatial synchrony in cisco recruitment. *Fisheries Research*, *165*, 11–21. https://doi.org/10.1016/j.fishres.2014.12.014

Myers, R. A. (1998). When do environment-recruitment correlations work? *Reviews in Fish Biology and Fisheries*, *8*(3), 285–305. https://doi.org/10.1023/A:1008828730759

Myers, R. A. (2001). Stock and recruitment: Generalizations about maximum reproductive rate, density dependence, and variability using meta-analytic approaches. *ICES Journal of Marine Science*, *58*(5), 937–951. https://doi.org/10.1006/jmsc.2001.1109

Myers, R. A., & Cadigan, N. G. (1993). Density-dependent juvenile mortality in marine demersal fish. *Canadian Journal of Fisheries and Aquatic Sciences*, *50*(8), 1576–1590. https://doi.org/10.1139/f93-179

Myers, R. A., Mertz, G., & Bridson, J. (1997). Spatial scales of interannual recruitment variations of marine, anadromous, and freshwater fish. *Canadian Journal of Fisheries and Aquatic Sciences*, *54*(6), 1400–1407. https://doi.org/10.1139/f97-045

Nicolau, P. G., Ims, R. A., Sørbye, S. H., & Yoccoz, N. G. (2022). Seasonality, density dependence, and spatial population synchrony. *Proceedings of the National Academy of Sciences of the United States of America*, *119*(51), e2210144119. https://doi.org/10.1073/pnas.2210144119

Olsen, E., Aanes, S., Mehl, S., Holst, J. C., Aglen, A., & Gjøsæter, H. (2010). Cod, haddock, saithe, herring, and capelin in the Barents Sea and adjacent waters: A review of the biological value of the area. *ICES Journal of Marine Science*, *67*(1), 87–101. https://doi.org/10.1093/icesjms/fsp229

Östman, Ö., Olsson, J., Dannewitz, J., Palm, S., & Florin, A. B. (2017). Inferring spatial structure from population genetics and spatial synchrony in demography of Baltic Sea fishes: Implications for management. *Fish and Fisheries*, *18*(2), 324–339. https://doi.org/10.1111/faf.12182

Ottersen, G., & Loeng, H. (2000). Covariability in early growth and year-class strength of Barents Sea cod, haddock, and herring: The environmental link. *ICES Journal of Marine Science*, *57*(2), 339–348. https://doi.org/10.1006/jmsc.1999.0529

Pauly, D. (1980). On the interrelationships between natural mortality, growth parameters, and mean environmental temperature in 175 fish stocks. *ICES Journal of Marine Science*, *39*(2), 175–192. https://doi.org/10.1093/icesjms/39.2.175

Pebesma, E. J. (2004). Multivariable geostatistics in {S}: The gstat package. *Computers & Geosciences*, *30*, 683–691.

Planque, B., Kristinsson, K., Astakhov, A., Bernreuther, M., Bethke, E., Drevetnyak, K., Nedreaas, K., Reinert, J., Rolskiy, A., Sigurðsson, T., & Stransky, C. (2013). Monitoring beaked redfish (*Sebastes mentella*) in the North Atlantic, current challenges and future prospects. *Aquatic Living Resources*, *26*(4), 293–306. https://doi.org/10.1051/alr/2013062

Planque, B., Loots, C., Petitgas, P., Ulf, L., & Vaz, S. (2011). Understanding what controls the spatial distribution of fish populations using a multi-model approach. *Fisheries Oceanography*, *20*(1), 1–17. https://doi.org/10.1111/j.1365-2419.2010.00546.x

Poloczanska, E. S., Brown, C. J., Sydeman, W. J., Kiessling, W., Schoeman, D. S., Moore, P. J., Brander, K., Bruno, J. F., Buckley, L. B., Burrows, M. T., Duarte, C. M., Halpern, B. S., Holding, J., Kappel, C. V., O'Connor, M. I., Pandolfi, J. M., Parmesan, C., Schwing, F., Thompson, S. A., & Richardson, A. J. (2013). Global imprint of climate change on marine life. *Nature Climate Change*, *3*(10), 919–925. https://doi.org/10.1038/nclimate1958

Poloczanska, E. S., Burrows, M. T., Brown, C. J., García Molinos, J., Halpern, B. S., Hoegh-Guldberg, O., Kappel, C. V., Moore, P. J., Richardson, A. J., Schoeman, D. S., & Sydeman, W. J. (2016). Responses of marine organisms to climate change across oceans. *Frontiers in Marine Science*, *3*(May), 1–21. https://doi.org/10.3389/fmars.2016.00062

Pörtner, H. O., & Peck, M. A. (2010). Climate change effects on fishes and fisheries: Towards a cause-and-effect understanding. *Journal of Fish Biology*, *77*(8), 1745–1779. https://doi.org/10.1111/j.1095-8649.2010.02783.x

Post, E., & Forchhammer, M. C. (2004). Spatial synchrony of local populations has increased in association with the recent northern hemisphere climate trend. *Proceedings of the National Academy of Sciences of the United States of America*, *101*(25), 9286–9290. https://doi.org/10.1073/pnas.0305029101

Sæther, B.-E., Engen, S., Grøtan, V., Fiedler, W., Matthysen, E., Visser, M. E., Wright, J., Møller, A. P., Balen, H. V. A. N., Balmer, D., Mark, C., Mccleery, R. H., Pampus, M., & Winkel, W. (2007). The extended Moran effect and large-scale synchronous fluctuations in the size of great tit and blue tit populations. *Journal of Animal Ecology*, *76*, 315–325. https://doi.org/10.1111/j.1365-2656.2006.01195.x

R Core Team. (2021). *R: A language and environment for statistical computing*. R Foundation for Statistical Computing. http://www.r-project.org/

Shepherd, T. D., & Litvak, M. K. (2004). Density-dependent habitat selection and the ideal free distribution in marine fish spatial dynamics: Considerations and cautions. *Fish and Fisheries*, *5*(2), 141–152. https://doi.org/10.1111/j.1467-2979.2004.00143.x

Stiansen, J. E., & Filin, A. A. (2008). Joint PINRO/IMR report on the state of the Barents Sea ecosystem in 2007, with expected situation and considerations for management. In *IMR-PINRO Joint Report Series 2008(1)* (Issue 3 (p. 185). Institute of Marine Research.

Sunday, J. M., Bates, A. E., & Dulvy, N. K. (2012). Thermal tolerance and the global redistribution of animals. *Nature Climate Change*, *2*(9), 686–690. https://doi.org/10.1038/nclimate1539

Thorson, J. T., Skaug, H. J., Kristensen, K., Shelton, A. O., Ward, E. J., Harms, J. H., & Benante, J. A. (2015). The importance of spatial models for estimating the strength of density dependence. *Ecology*, *96*(5), 1202–1212. https://doi.org/10.1890/14-0739.1

Turkia, T., Jousimo, J., Tiainen, J., Helle, P., Rintala, J., Hokkanen, T., Valkama, J., & Selonen, V. (2020). Large-scale spatial synchrony in red squirrel populations driven by a bottom-up effect. *Oecologia*, *192*(2), 425–437. https://doi.org/10.1007/s00442-019-04589-5

Viboud, C., Bjørnstad, O. N., Smith, D. L., Simonsen, L., Miller, M. A., & Grenfell, B. T. (2006). Synchrony, waves, and spatial hierarchies in the spread of influenza. *Science*, *312*(5772), 447–451. https://doi.org/10.1126/science.1125237

Vindstad, O. P. L., Jepsen, J. U., Yoccoz, N. G., Bjørnstad, O. N., Mesquita, M. D. S., & Ims, R. A. (2019). Spatial synchrony in sub-arctic

13652656, 2023, 11, Downloaded from https://besjournals.onlinelibrary.wiley.com/doi/10.1111/1365-2656.14008 by Institute Of Marine Research, Wiley Online Library on [21/11/2023]. See the Terms and Conditions (https://onlinelibrary.wiley.com/terms-and-conditions) on Wiley Online Library for rules of use; OA articles are governed by the applicable Creative Commons License

geometrid moth outbreaks reflects dispersal in larval and adult life cycle stages. *Journal of Animal Ecology*, *88*(8), 1134–1145. https://doi.org/10.1111/1365-2656.12959

Walter, J. A., Sheppard, L. W., Anderson, T. L., Kastens, J. H., Bjørnstad, O. N., Liebhold, A. M., & Reuman, D. C. (2017). The geography of spatial synchrony. *Ecology Letters*, *20*(7), 801–814. https://doi.org/10.1111/ele.12782

SUPPORTING INFORMATION

Additional supporting information can be found online in the Supporting Information section at the end of this article.

Figure S1: Estimated average annual sea bottom temperature (sea bottom to 30 m above sea bottom) between January to April.

Figure S2: Maps showing the estimated local log-densities each year. The solid lines around the coloured cells show that total area that was sampled that year, with white space showing areas that had been sampled but no individuals of the species were found. The dotted lines show the total area where the species has been found at least once during the duration of the survey. The grey areas show the land masses surrounding the Barents Sea.

Figure S3: Gaussian variograms showing the spatial autocorrelation for each species (noted on the top left) in density by year. The solid variogram line shows the autocorrelation in density, and the dashed line shows the results of the autocorrelation in the residual density after estimating the predicted effect that temperature had on density each year. The values on the top left of each plot show the range (km) and the sill of the density (top) and residual density (bottom).

Figure S4: Maps of the Barents Sea with the hexagonal grid used to define each site. The colors represent the regression coefficient (β) of the variables used to estimate local density growth, i.e. strength of density dependence and sea bottom temperature, SBT. These regression coefficients correspond to the ones obtained when modelling local density growth with either variable independently. Lower β in the density regulation represent stronger density dependence. The outer grey polygon represents the sites in which the species have been caught at least once, however, only sites with more than five data points were included. The inner black polygon shows the sites where there was data for both density changes and temperature.

Figure S5: Spatial synchrony in annual density changes. Each column represents the spatial synchrony corresponding to the residuals of the model which included the variable or variables noted on the right. That is, the synchrony in the local density changes not explained by that variable. The black solid and dotted lines in each plot represent the median and 95% confidence intervals of the spatial synchrony of the unaltered annual density changes for the corresponding species, and its included for easier comparison. The resolutions under which the analyses were performed in shown at the top.

How to cite this article: Marquez, J. F., Herfindal, I., Sæther, B.-E., Aanes, S., Salthaug, A., & Lee, A. M. (2023). Effects of local density dependence and temperature on the spatial synchrony of marine fish populations. *Journal of Animal Ecology*, *92*, 2214–2227. https://doi.org/10.1111/1365-2656.14008

13652656, 2023, 11, Downloaded from https://besjournals.onlinelibrary.wiley.com/doi/10.1111/1365-2656.14008 by Institute Of Marine Research, Wiley Online Library on [21/11/2023]. See the Terms and Conditions (https://onlinelibrary.wiley.com/terms-and-conditions) on Wiley Online Library for rules of use; OA articles are governed by the applicable Creative Commons License